The role of membrane microdomains in shaping β_2-adrenergic receptor-mediated cAMP dynamics†

Lisa M. DiPilato[a] and Jin Zhang*[ab]

Received 24th December 2008, Accepted 8th April 2009
First published as an Advance Article on the web 26th May 2009
DOI: 10.1039/b823243a

Recently, membrane rafts and caveolae have received much attention for their role as signaling platforms, particularly due to their involvement in the pathogenesis of a number of diseases, including HIV as well as neurological and cardiovascular conditions. Signaling mediated by the β-adrenergic receptor (β-AR), a member of the large family of G-protein coupled receptors (GPCRs) that transduce extracellular messages *via* the ubiquitous second messenger, cAMP, has been a focus of raft studies since multiple components of the pathway are compartmentalized by these membrane microdomains. However, how these membrane rafts behave and regulate signaling dynamics in a cellular context is poorly understood. Here, we describe a live-cell assay based on single-cell, real-time fluorescence imaging, *via* an improved FRET-based cAMP biosensor, to monitor raft regulation of second messenger dynamics. Upon cholesterol depletion with methyl-β-cyclodextrin (MβCD), β_2-AR-mediated cAMP accumulation was enhanced and prolonged in HEK-293 cells, demonstrating that membrane raft integrity helps shape β-AR signaling. Single-cell imaging in parallel with fractionation studies reveal that the enhancement and change of dynamics are mediated by the receptor and correlated with its redistribution. Finally, the effect of cholesterol depletion is receptor-type specific as MβCD treatment did not show the same effect when the raft-excluded prostaglandin E receptor was stimulated. This study highlights the potential of a live-cell, real-time imaging assay for studying membrane rafts, including high sensitivity and spatiotemporal resolution, to achieve a better understanding of the nuances of membrane microdomains in both healthy and diseased states.

Introduction

Membrane rafts, including caveolae, are "small (10–200 nm), heterogeneous, highly dynamic" microdomains that are enriched in cholesterol and sphingolipids.[1] The combined structural and physical characteristics of these sterols and lipids give rise to regions in the membrane that are highly ordered and less fluid, a stark contrast to the more disordered, fluid (non-raft) membrane environment. Functionally, these microdomains have been implicated in the regulation of cellular processes including signal transduction, endocytosis, trafficking and viral entry, assembly and budding.[2] Specifically, the partitioning of receptors and other signaling components into different compartments of the membrane has been shown to be integral for achieving specificity.[3,4] For example, components of a pathway can co-localize within rafts to enhance signaling efficiency, while segregation of components into different compartments can regulate basal activity and direct a signal to follow a specific transduction route.[5] Moreover, membrane rafts and caveolae have been connected with a growing number of health conditions such as neurological and cardiovascular diseases, making them an exciting target for new therapeutics.[6]

Cyclic AMP (cAMP) is a ubiquitous second messenger that governs many cellular processes with high specificity, fidelity and efficiency. A model of second messenger signaling, cAMP is generated by G protein coupled receptor (GPCR)-mediated activation of adenylyl cyclase (AC) *via* G_α stimulatory proteins and goes on to elicit highly specific cellular responses through only a few effector proteins: cAMP dependent protein kinase (PKA), exchange protein directly activated by cAMP (Epac) and cyclic nucleotide gated (CNG) channels.[7] It is believed that compartmentation, for example spatial compartmentation within membranes, is a necessary mechanism for achieving this specificity.[8] In fact, cAMP pathway components, including GPCRs, specifically adrenergic (β_1- and β_2-AR), cholinergic (mAChR and nAChR), and angiotensin receptors (AT_1-R), as well as AC, G_α proteins, phosphodiesterases and effector molecules, such as CNG channels, have been shown to dynamically associate with membrane rafts/caveolae in a variety of tissues and cell types (see ref. 9 for individual references). Yet how the specific distribution of these pathway components regulates signaling specificity is not yet completely understood.

Membrane rafts have remained difficult to study due to their intrinsic properties: size, heterogeneity and dynamic nature. Biochemical approaches for isolating membrane rafts *via* fractionation have enabled the study of lipid composition

[a] *Department of Pharmacology and Molecular Sciences, The Johns Hopkins University School of Medicine, Maryland*
[b] *Departments of Neuroscience and Oncology, The Johns Hopkins University School of Medicine, Maryland*
† Electronic supplementary information (ESI) available: Supplementary figures. See DOI: 10.1039/b823243a

and protein localization within these compartments, however this method provides only snap shots of dynamic signaling and removes signaling components from their live-cell context.[5] Moving towards more *in vivo* analysis, fluorescence resonance energy transfer (FRET) experiments have been used to monitor specific proteins in these microdomains in living cells.[10] When combined with these techniques, pharmacological disruptors of membrane rafts such as cholesterol depleting agents (cyclodextrins and filipin) and cholesterol synthesis inhibitors have been useful for probing the functional consequences of these microdomains, such as their role in regulating CNG channel activity.[11] While these techniques have led to important findings regarding membrane rafts, more sensitive and dynamic tools are needed to study their regulation of signaling dynamics in their native environment.

We have successfully developed biosensors for studying the spatiotemporal dynamics of second messenger signaling in single living cells in real-time using fluorescence microscopy. Indicator of cAMP using Epac (ICUE) was designed by sandwiching Epac1, a guanine exchange factor for the small GTPase Rap1, between two green fluorescent protein (GFP) variants. Upon cAMP binding, the protein undergoes a conformational change resulting in a decrease in fluorescence resonance energy transfer (FRET).[12] Multiple cAMP biosensors have been developed[13] and the broad application of such dynamic sensors to monitor second messenger dynamics have been reported in a variety of cells types and using different assay platforms.[14–16] Given the benefits of these biosensors, we set out to study the role of membrane microdomains in regulating β-adrenergic-mediated cAMP dynamics in HEK-293 cells using these tools and live-cell imaging.

Results

ICUE3 and lynICUE3 characterization

In order to monitor cAMP dynamics in living cells, we have developed a series of Epac-based biosensors, ICUEs, that are able to sensitively detect cAMP production and degradation in real-time.[12,16] In order to achieve a good signal-to-noise ratio, it is desirable to have a sensor with a large dynamic range that is suitable for detecting subtle or suboptimal changes that are physiologically relevant. Furthermore, subcellular localization tags on such reporters can sometimes negatively impact the overall dynamic range presumably due to a constraint in the conformational change of the sensor itself. For example, targeting ICUE2 to the plasma membrane *via* a farnesylation modification consensus sequence diminished the dynamic range of ICUE2 by about half (Fig. 1A&C). Previous FRET-based sensors have been shown to be improved upon the introduction of circularly permuted fluorescent proteins.[17] Following this strategy, we exchanged our current FRET acceptor, citrine, in ICUE2 with circularly permuted YFP variants, cpVenus, at residues K156, E172 and L194 as well as wild type Venus.

Single cell imaging studies revealed cpVenus at residue L194 gave the largest dynamics range, a maximum percent ratio change of 102.2 ± 2.9% (n = 11) [average ± SEM,

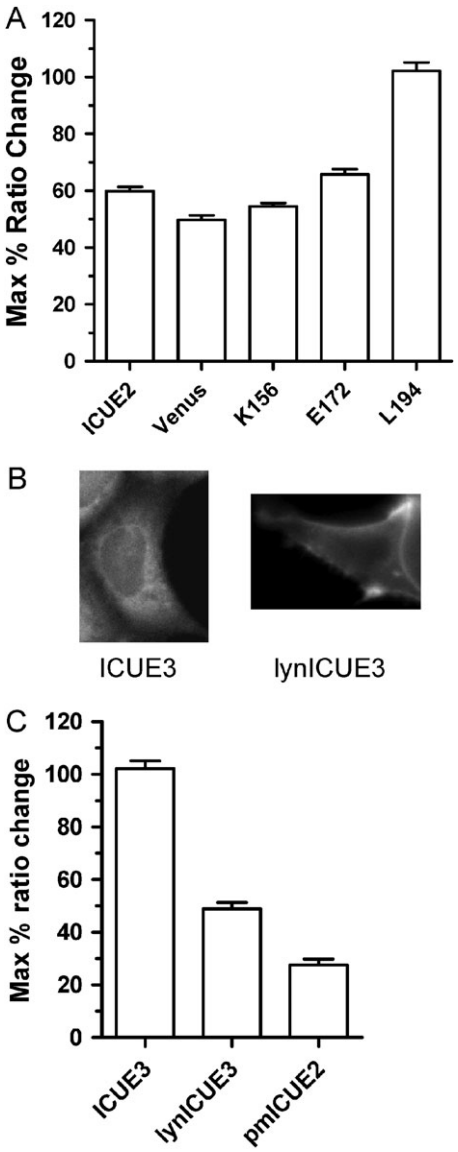

Fig. 1 Characterization of ICUE3 in HEK-293 cells. (A) Bar graph of maximum percent ratio changes for ICUE2 and cpVenus variant-containing ICUE2 sensors. (B) CFP images of ICUE3 (cpVL194) and lynICUE3. (C) Comparison of average maximum percent ratio changes for ICUE3, lynICUE3 and pmICUE2.

n = number of cells] upon stimulation of AC with 50 μM forskolin (Fsk) in HEK-293 cells. This probe, we refer to as ICUE3, has a 67% improvement over ICUE2 (Fig. 1A). Like ICUE2, ICUE3 is expressed diffusely throughout the cytosol and excluded from the nucleus when transfected into HEK-293 cells. Also, we effectively targeted ICUE3 to the plasma membrane using a myristoylation and palmitoylation sequence from Lyn kinase to measure cAMP closer to the site of its generation (Fig. 1B). Furthermore, this targeting sequence has been shown to localize proteins to the raft regions of membranes.[18] Similar to the improvement of ICUE3 over ICUE2, this version of Lyn sequence targeted ICUE3 (lynICUE3) showed a 63% improvement over plasma membrane ICUE2 (pmICUE2) upon 50 μM Fsk addition (49.0 ± 2.4%, n = 4 compared to 27.6 ± 2.3% n = 9)

(Fig. 1C). Thus, the improved dynamic range of ICUE3 enabled the generation of a membrane targeted biosensor, lynICUE3, with a much improved dynamic range over previous targeted versions.

Cholesterol depletion enhances cAMP production and prolongs response in HEK-293 cells

Having improved the reporter and demonstrated its ability to sensitively monitor cAMP dynamics at the plasma membrane, we turned our attention to the role of membrane microdomains in shaping cAMP dynamics. We used isoproterenol, a β-adrenergic agonist which effectively generates cAMP *via* activation of the β_2-AR in HEK-293 cells. In control cells, addition of 1 μM Iso generated a submaximal (49.9 ± 4.7%, n = 22), transient response measured as an increase in cyan emission to yellow emission upon cyan excitation (Fig. 2A).

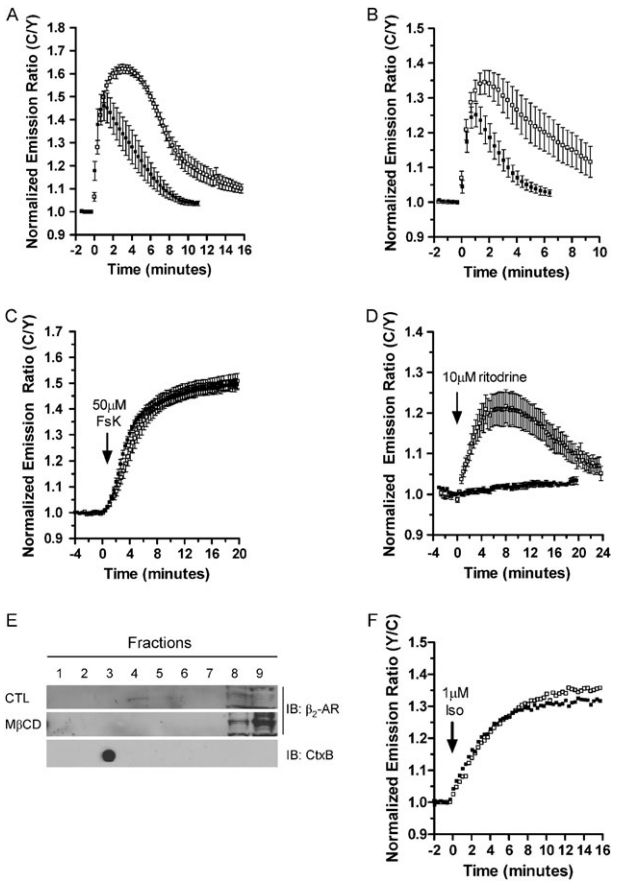

Fig. 2 Enhancement of β_2-AR-mediated cAMP accumulation in HEK-293 cells upon cholesterol depletion. Average emission ratio time courses of ICUE3 (A) and lynICUE3 (B) upon stimulation with 1 μM Iso ± 10 mM MβCD. (C&D) Average emission ratio time course of lynICUE3 response upon addition of 50 μM Fsk (C) and 10 μM ritodrine (D) ±pretreatment of cells with 10 mM MβCD. (E) Western analysis of β_2-AR localization in membrane fractionations of HEK-293 cells ± 10 mM MβCD treatment. (F) Average emission ratio time course of β_2-AR-CFP/β-arrestin2-YFP bimolecular reporter upon addition of 1 μM Iso ± 10 mM MβCD treatment. All time course data are presented as average ±SEM. Cells pretreated with MβCD are represented as open squares (□) and untreated as closed squares (■).

Using cholesterol depletion to disrupt membrane rafts,[19] we pre-treated HEK-293 cells expressing ICUE3 with 10 mM MβCD for 30 min followed by stimulation with 1 μM Iso. Cholesterol depletion resulted in an enhanced cAMP response of 62.9 ± 1.9% (n = 93), 26% greater than cells treated with Iso alone, consistent with previous studies using cAMP assays.[20–22] Furthermore, cells pretreated with MβCD took almost twice as long as untreated cells to reach maximum upon β_2-AR stimulation ($t_{1/2}$ = 26 ± 3s (n = 93) and 15 ± 3 s (n = 22), respectively), and longer to return to baseline (Fig. 2A). This effect is also dose-dependent as 100 nM Iso-stimualtion after cholesterol depletion resulted in a more subtle effect (Fig. S1†) Cholesterol depletion showed a similar trend in enhanced amplitude and prolonged response with the plasma membrane targeted version, lynICUE3 (Fig. 2B). We performed the rest of our experiments with lynICUE3 to monitor cAMP dynamics at the plasma membrane.

The methyl β-cyclodextrin effect is dependent on the receptor and its localization within the membrane

To explore the effect of membrane raft disruption on β_2-AR signaling further, we set out to determine if cholesterol depletion affected other pathway components in the membrane. To this end, we treated lynICUE3-expressing HEK-293 cells with MβCD and bypassed the receptor by directly stimulated AC with 50 μM Fsk. We observed no statistical difference in either amplitude or kinetics between treated and untreated cells (Fig. 2C). These results suggest the MβCD-mediated enhancement of cAMP response is receptor-dependent. To confirm this, we stimulated cells with another β_2-AR ligand, ritodrine. Ritodrine is known to have partial agonist properties and we were unable to detect a cAMP response with ICUE upon addition of the drug due to this diminished efficacy. However, upon pretreatment with 10 mM MβCD, 10 μM ritodrine elicited a robust response with a maximum ratio change of 21.8 ± 3.9% (n = 3) similar to the enhancement observed for 1 μM Iso (Fig. 2D). The cholesterol depletion effect for ritodrine appears more dramatic since the amount of cAMP produced with 10 μM ritodrine alone is beyond the detection limit of the sensor. This dramatic enhancement in ritodrine-mediated cAMP response upon cholesterol depletion confirms the effect is receptor-dependent and not agonist dependent.

Next, we performed membrane fractionation using a sucrose density gradient method in order to determine the localization of endogenous β_2-AR in HEK-293 cells before and after treatment with MβCD. Nine fractions were taken, from low density, buoyant fractions to higher density fractions (1–9, respectively). Membrane rafts localize to the more buoyant fraction, whereas non-raft regions are localized to higher density fractions. Membrane raft marker Cholera toxin B subunit (CtxB), which binds to a known raft-associated ganglioside, GM1, indicated that raft regions were found to be in fraction 3. Upon probing these fractions with a β_2-AR specific antibody, endogenous β_2-AR was detected in fractions 4 and 5 without any treatments. Upon cholesterol depletion, the bands disappeared from these fractions, consistent with

redistribution of the receptor throughout the membrane (Fig. 2E). As a control, we determined the localization of lynICUE3 using the same method. LynICUE3 was found in fractions 3 and 4 as well as in fractions 8 and 9, showing partial lipid raft targeting. Upon treatment with MβCD, some redistribution among the fractions was observed (Fig. S2†). And since we see similar MβCD-mediated effects between the plasma membrane and the untargeted probe upon 1 μM Iso stimulation, we can conclude that the redistribution of the receptor is having a global effect on cAMP dynamics under this condition.

Studies in cardiomyocytes have shown that caveolae are important for proper desensitization of the β_2-AR.[20,23] We have previously shown that receptor desensitization, particularly homologous desensitization mediated by G protein coupled receptor kinase (GRK) and β-arrestin, is an important mechanism in shaping cAMP dynamics in HEK-293 cells.[16] Thus, we set out to probe the effect of cholesterol depletion on desensitization using a bimolecular FRET-based probe of β-arrestin recruitment. The probe, consisting of a CFP-tagged β_2-AR and a YFP-tagged β-arrestin2, reports β-arrestin recruitment to the receptor as an increase in FRET. This FRET increase is highly dependent on GRK phosphorylation of the receptor, as siRNA against GRK isoforms has been shown to significantly reduce the observed rate (k_{obs}) of response.[24] Thus, if GRK phosphorylation and β-arrestin recruitment were perturbed upon membrane raft disruption, we would expect to see a difference in the kinetic parameters ($t_{1/2}$) of the response curve. Upon stimulation of HEK-293 cells stably expressing both reporter components with 1 μM Iso, we observed an increase in emission ratio of YFP to CFP as expected. However, we observed no perturbation of the rate of response upon pretreatment with 10 mM MβCD, indicating GRK phosphorylation and β-arrestin recruitment is unaltered by the treatment (Fig. 2F).

Membrane raft disruption effect is receptor-type specific

It is known that GPCRs differentially localize within the membrane. For example, the G_s-coupled prostaglandin E receptors, EP2-R and EP4-R, have been shown consistently to be excluded from membrane rafts in mammalian cells. We confirmed the localization of the EP2-R in the less ordered, non-raft region in the membrane of HEK-293 cells *via* sucrose density gradient membrane fractionation. Western analysis of the fractions revealed the presence of EP2-R in the higher density fractions (7–9) which did not change significantly upon MβCD treatment (Fig. 3A). In HEK-293 cell expressing lynICUE3, we observed no statistical difference in maximum cAMP response between MβCD treated (13.8 ± 2.3%, n = 8) and untreated cells (14.6 ± 2.1%, n = 12) upon stimulation of EP-R with 1 μM PGE_1 (Fig. 3B). However, cholesterol depletion elicited a faster response ($t_{1/2}$ = 51.5 ± 2.8 s, n = 8 compared to $t_{1/2}$ = 66.9 ± 5.4 s, n = 12; p value = 0.0224) (Fig. 3C). The slightly faster EP-R-mediated response is the opposite effect seen for β_2-AR. These results suggest the cholesterol depletion effect is highly dependent on receptor localization within the membrane and its redistribution.

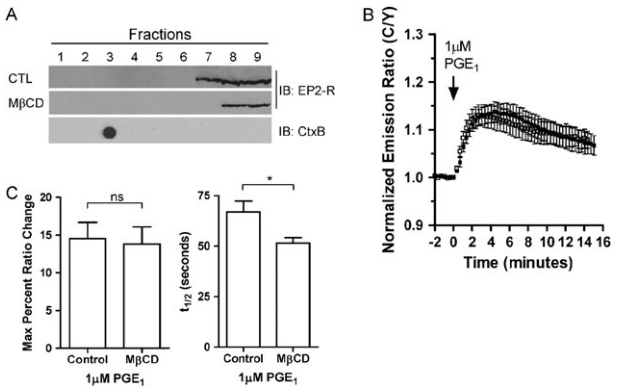

Fig. 3 The MβCD effect is receptor-specific. (A) Western analysis of EP2-R localization in membrane fractions from HEK-293 cells ±10 mM MβCD treatment. (B) Emission ratio time courses of lynICUE3 upon addition of 1 μM PGE_1 with (□) or without (■) 10 mM MβCD pretreatment. (C) Comparison of the maximum percent ratio change and $t_{1/2}$ values. All data are presented as average ±SEM.

Discussion

β_2-AR is a prototypical GPCR which has been shown to have distinct localization within membrane microdomains in different cell types. Using an improved cAMP biosensor in live cells, we detect an enhanced isoproterenol-mediated cAMP accumulation and prolonged response upon disruption of membrane rafts *via* cholesterol depletion. However, this result was only observed for the raft-associated β_2-AR. The EP-R, which resides in the non-raft regions of the membrane, showed no enhanced cAMP response upon cholesterol depletion. In fact, we observed somewhat faster accumulation of cAMP. We can conclude that membrane rafts negatively regulate β_2-AR signaling in addition to known feedback mechanisms. And this regulation is highly dependent on receptor localization within these microdomains. It is of note that compartmentation was first proposed to help explain the functional differences between Iso- and PGE_1-mediated signaling in cardiomyocytes.[7] It is therefore conceivable that the assay described here can be applied to explore this functional difference in terms of membrane rafts.

Our observations are consistent with a recent study involving the biochemical analysis of the same receptor using AC activity assays to measure cholesterol depletion effects on cAMP production.[21] Interestingly, Pontier *et al.* report MβCD treatment enhances Fsk-mediated cAMP production. However, in our live-cell imaging assay, we did not observe such effect of cholesterol depletion using the same concentration of Fsk. This discrepancy may be due to the different readout, AC activity *versus* accumulation of free cAMP, as well as other differences inherent in these two assays, and highlights the importance of employing complementary approaches to studying signal transduction within membrane microdomains in order to obtain an accurate understanding of what is occurring within the cell.

This study illustrates the potential of a live-cell, real-time imaging assay for studying membrane microdomains. First, FRET-based imaging enables the measurement of signaling dynamics within live cells with high temporal resolution.

As demonstrated with ICUE, we were able to monitor the effect of cholesterol depletion not only at a specific time point, but in real-time as cells were responding. Besides free cAMP concentration, we were able to monitor rate of cAMP accumulation and duration of response as well as subtle changes to these kinetic parameters. Furthermore, specific targeting of these biosensors allows the direct measurement of raft and non-raft signaling kinetics. For example, we recently showed a FRET-based Akt activity probe, AktAR, is able to detect differential growth factor signaling within these membrane microdomains.[18] Thus, this assay can be generally applicable to study the roles of membrane microdomains in regulating other receptors and pathways, providing rich information that is difficult, if not impossible, to obtain by other assays.

Experimental

Development and targeting of ICUE3

ICUE3 was developed by excising citrine from ICUE2[16] in pcDNA3 vector and replacing it with circularly permuted variant of yellow fluorescent protein (YFP), Venus, at residue L194 using SacI and EcoRI restriction sites. ICUE3 was targeted to the plasma membrane *via* a myristoylation and palmitoylation lipid modification consensus sequence (GCIKSKRKDKD).

Cell culture

HEK-293 cells were maintained in DMEM (10% FBS and 1% pen/strep) at 37 °C with 5% CO_2. For imaging, cells were plated onto sterilized glass coverslips in 35 mm dishes transfected with FuGENE-6 transfection reagent (Roche) or calcium phosphate at 50–60% confluence and allowed to grow for 18–24 h before imaging.

Imaging

Cells were washed twice with and maintained in Hanks' balanced salt solution (HBSS) buffer and allowed to equilibrate for 10 min at room temperature in the dark. Cells were treated with isoproterenol (ISO; Aldrich), PGE_1 (Sigma), and forskolin (Fsk; Calbiochem) as indicated. For cholesterol depletion experiments, cells were treated with 10 mM methyl-β-cyclodextrin (MβCD; Sigma) for 30 min at 37 °C and then washed 2–3 times with HBSS imaging buffer before imaging.

Dual emission ratio imaging was performed on a Zeiss Axiovert 200 M microscope with a MicroMAX BFT512 cooled charge-coupled device camera (Roper Scientific, Trenton, NJ) controlled by METAFLUOR 6.2 software (Universal Imaging, Downingtown, PA). Emission ratios were obtained using a 420DF20 excitation filter, a 450DRLP dichroic mirror, and two emission filters (475DF40 for ECFP and 535DF25 for citrine) alternated by a Lambda 10–2 filter-changer (Sutter Instruments, Novato, CA). Images were taken every 20 s with an exposure time of 100–500 ms. Fluorescent images were background-corrected by subtracting autofluorescence intensities of untransfected cells (or background with no cells) from the emission intensities of cells expressing reporters.

Sucrose density gradient fractionation and western analysis

Isolation of detergent resistant membranes from HEK-293 cells was achieved by sucrose density gradient fractionation as previously described.[18] Individual fractions were run on a 10% SDS-polyacrylamide gel electrophoresis (PAGE) and transferred to nitrocellulose membranes. β_2-AR and EP2-R were detected by immunoblotting with antibodies from Santa Cruz and Cell Signaling, respectively. LynICUE3 was detected by immunoblotting with a anti-GFP and GFP mutant fusion proteins antibody from eBioscience. For determining location of raft regions, the fractions were dot blotted on nitrocellulose membrane and probed with HRP conjugated Cholera toxin subunit B (CTxB) antibody.[18] Chemiluminescence detection was performed with horseradish peroxidase-conjugated secondary antibody and SuperSignal West Pico reagent (Pierce).

Conclusion

Employing an improved FRET-based cAMP biosensor (ICUE3) and live-cell real-time fluorescence imaging, we were able to test the role of membrane raft integrity in shaping β_2-AR-mediated cAMP signaling upon their disruption *via* cholesterol depletion. This assay is an important addition to the current tool kit for studying the biological significance of these dynamic and often elusive membrane microdomains with high sensitivity and resolution and can be readily applied to the studies of different receptors in various cell types.

Acknowledgements

We would like to thank Drs David Zukerman and Carolyn Machamer for help with sucrose density gradient fractionation, Dr Robert J. Lefkowitz for providing us with the β-arrestin recruitment FRET probe and Qiang Ni and Dr Xinxin Gao for critical reading of the manuscript. This work is funded by NIH R01 DK073368, the Young Clinical Scientist Award Program of the Flight Attendant Medical Research Institute, a Scientist Development Award from the American Heart Association, and 3M (to J. Z.) and F31 DK074381 (L.M.D).

References

1 L. J. Pike, *J. Lipid Res.*, 2006, **47**, 1597–1598.
2 L. J. Pike, *Biochem. J.*, 2004, **378**, 281–292.
3 B. Chini and M. Parenti, *J. Mol. Endocrinol.*, 2004, **32**, 325–338.
4 K. Simons and D. Toomre, *Nat. Rev. Mol. Cell Biol.*, 2000, **1**, 31–39.
5 L. J. Pike, *J. Lipid Res.*, 2003, **44**, 655–667.
6 V. Michel and M. Bakovic, *Biol. Cell*, 2007, **99**, 129–140.
7 R. Kopperud, C. Krakstad, F. Selheim and S. O. Doskeland, *FEBS Lett.*, 2003, **546**, 121–126.
8 I. L. Buxton and L. L. Brunton, *J. Biol. Chem.*, 1983, **258**, 10233–10239.
9 D. Willoughby and D. M. Cooper, *Physiol. Rev.*, 2007, **87**, 965–1010.
10 P. Sharma, R. Varma, R. C. Sarasij, s. Ira, K. Gousset, G. Krishnamoorthy, M. Rao and S. Mayor, *Cell*, 2004, **116**, 577–589.
11 J. D. Brady, T. C. Rich, X. Le, K. Stafford, C. J. Fowler, L. Lynch, J. W. Karpen, R. L. Brown and J. R. Martens, *Mol. Pharmacol.*, 2004, **65**, 503–511.

12 L. M. DiPilato, X. Cheng and J. Zhang, *Proc. Natl. Acad. Sci. U. S. A.*, 2004, **101**, 16513–16518.
13 D. Willoughby and D. M. Cooper, *Nat. Methods*, 2008, **5**, 29–36.
14 V. O. Nikolaev, M. Bunemann, E. Schmitteckert, M. J. Lohse and S. Engelhardt, *Circ. Res.*, 2006, **99**, 1084–1091.
15 M. D. Allen, L. M. DiPilato, M. Rahdar, Y. R. Ren, C. Chong, J. O. Liu and J. Zhang, *ACS Chem. Biol.*, 2006, **1**, 371–376.
16 J. D. Violin, L. M. DiPilato, N. Yildirim, T. C. Elston, J. Zhang and R. J. Lefkowitz, *J. Biol. Chem.*, 2007, **283**, 2949–2961.
17 T. Nagai, S. Yamada, T. Tominaga, M. Ichikawa and A. Miyawaki, *Proc. Natl. Acad. Sci. U. S. A.*, 2004, **101**, 10554–10559.
18 X. Gao and J. Zhang, *Mol. Biol. Cell*, 2008, **19**, 4366–4373.
19 R. Zidovetzki and I. Levitan, *Biochim. Biophys. Acta, Biomembr.*, 2007, **1768**, 1311–1324.
20 V. O. Rybin, X. Xu, M. P. Lisanti and S. F. Steinberg, *J. Biol. Chem.*, 2000, **275**, 41447–41457.
21 S. M. Pontier, Y. Percherancier, S. Galandrin, A. Breit, C. Galés and M. Bouvier, *J. Biol. Chem.*, 2008, **283**, 24659–24672.
22 Y. Miura, K. Hanada and T. L. Jones, *Biochemistry*, 2001, **40**, 15418–15423.
23 R. S. Ostrom, C. Gregorian, R. M. Drenan, Y. Xiang, J. W. Regan and P. A. Insel, *J. Biol. Chem.*, 2001, **276**, 42063–42069.
24 J. D. Violin, X. R. Ren and R. J. Lefkowitz, *J. Biol. Chem.*, 2006, **281**, 20577–20588.